

Comparison of Solar Module Damage Texture Analysis using GLCM and LBP

Widya Tari

Department of Informatics Engineering, Institut Teknologi
Perusahaan Listrik Negara, Jakarta, Indonesia

Rizqia Cahyaningtyas

Department of Informatics Engineering, Institut Teknologi
Perusahaan Listrik Negara, Jakarta, Indonesia

Abstract: Solar modules play a vital role in renewable energy systems by converting sunlight into electrical energy. Over time, the surface of the panels can develop various issues such as cracks, scratches and stains, leading to a reduction in efficiency and energy output. Manual inspections have limitations in terms of time and cost; therefore, a solar panel damage detection system is required, utilising a reliable method for image analysis. The data used to test the model comprised 24 solar modules images, sourced from primary and secondary data. The collected images represent both physical and electrical damage. The methods used for feature extraction utilised the Gray Level Co-occurrence Matrix (GLCM) and Local Binary Pattern (LBP) techniques. GLCM features were calculated at four different angles (0° , 45° , 90° , and 135°), incorporating metrics such as contrast, dissimilarity, homogeneity, energy, and ASM, whilst LBP features were extracted using metrics such as mean, variance, and entropy. The process continued with damage segmentation of the images using Otsu Thresholding to calculate the proportion of damaged area. The results of the study show that the largest detected damaged area reached 35% for GLCM and 27% for LBP. These results indicate that GLCM is more effective in class separation, whilst LBP is capable of capturing local texture patterns. This model has the potential to support the automatic maintenance of solar panels and improve the efficiency of solar energy utilisation.

Keywords: texture analysis, GLCM, LBP, solar module, segmentation.

Correspondents Author:

Widya Tari, Department of Informatics Engineering, Institut Teknologi Perusahaan Listrik Negara, Jakarta, Indonesia
Email: widya2231028@itpln.ac.id

Received February 6 2026; Revised April 21, 2026; Accepted April 22, 2026; Published April 23, 2026.

Introduction

Machine Learning (ML) technology is often used as a practical empirical approach for regression and classification. ML algorithms can model complex classes with high accuracy because they accept various input variables without making specific assumptions about data distribution. Texture features in remote sensing are manifested in the form of spatial correlations, which are estimated through statistical techniques in moving windows of different sizes ([Zhang et al., 2017](#)). The Gray Level Co-occurrence Matrix (GLCM) method is a statistical technique often used to extract texture features. This technique provides information about the spatial intensity relationships between pixels, enabling the identification of patterns associated with different surface conditions ([Punnappurath et al., 2024](#); [Rai et al., 2026](#)).

The GLCM method is commonly used to create texture features from images. Several texture measures obtained from GLCM include mean, variance, homogeneity, contrast, entropy, correlation, and dissimilarity. Previous studies on land cover and land use classification have shown that using texture variables calculated through GLCM can provide additional information that helps improve classification results ([Wen et al., 2026](#)). GLCM is used to extract texture features to identify small cracks in photovoltaic modules, and shows a good level of accuracy in a controlled environment. A combined approach using GLCM and support vector machines (SVM) was used to classify damage types, yielding good results with various types of datasets. Texture features based on histograms were applied to distinguish between cracks and sunburn on solar modules, confirming that selecting the right features is crucial in improving classification accuracy ([Ali et al., 2025](#)). The GLCM can identify complex texture qualities in images. This metric provides a quantitative description of texture features and provides useful information about the spatial correlation between pixel intensities ([Subeesh & Chauhan, 2025](#)). The GLCM, which is a texture analysis technique for images. GLCM represents the relationship between two neighboring pixels based on grayscale intensity, distance, and angle. There are 8 angles that can be used in GLCM, namely 0° , 45° , 90° , 135° , 180° , 225° , 270° , or 315° ([Subeesh & Chauhan, 2025](#)). Based on research ([Kiswanto et al., 2024](#)), The GLCM is a statistical method used to analyze how pixels in an image are adjacent to each other. GLCM creates a matrix that shows how often gray color combinations appear within a certain distance and direction. A texture analysis metric similar to GLCM is Local Binary Pattern (LBP). LBP analyzes texture patterns around each pixel by comparing the gray values of surrounding pixels. Like GLCM, various mathematical features describing the image structure are calculated ([Cahyaningtyas et al., 2025](#)). LBP is widely used in the fields of surveillance and security. Additionally, LBP is also used in texture color description and face recognition. LBP is a statistical method that can efficiently summarize the local structure of

an image by comparing each pixel with its neighbors. Using LBP, images can be easily displayed based on two complementary measures, namely “local pattern” and “gray scale contrast” ([Wan et al., 2017](#)). LBP is calculated by connecting the bits of integers with their neighbors. If the intensity of a neighboring pixel is higher than the pixel being processed, then that bit will have a value of 1. Until a binary matrix is obtained, pixels whose intensity is less than the threshold value will be represented as 0 in binary form, while pixels whose intensity is greater than or equal to the threshold value will be given a value of 1 in binary form. Each neighboring pixel is connected to a part of one bit, resulting in $2^8 = 255$ neighbor combinations for a 3×3 matrix (8 neighbors). The resulting binary values are written directly from right to left in binary string form. The operations performed on each binary row are then combined to obtain the entire texture data ([Dhanraj et al., 2021](#)). The LBP technique is a commonly used method for describing texture in image processing and computer vision. This method is a simple yet efficient way to reveal texture characteristics within an image. The LBP feature extraction process is carried out in stages by comparing each pixel with its surrounding pixels ([Dheepak et al., 2024](#)). One application using GLCM and LBP is to determine damage to solar modules.

Solar modules consist of several solar cells arranged in series and parallel to generate electrical energy as needed. Each solar cell typically has a voltage of around 0.6 volts. To obtain the appropriate voltage, solar cells are usually arranged in series. The number of sheets used is usually 36 or 72, so that they can meet the needs of 12-volt and 24-volt systems ([Kiswanto et al., 2024](#)). In general, solar modules can last for 20 to 25 years, especially for monocrystalline modules ([Barburiceanu et al., 2021](#)). Solar modules are an important part of renewable energy systems that convert sunlight into electricity. However, their efficiency can decrease over time due to damage to the surface, such as cracks, scratches, or stains, which block sunlight and reduce the ability to convert energy. Thus, monitoring and analyzing the condition of the solar module surface is very important to maintain optimal performance. Maintenance using manual inspection methods is usually time-consuming and prone to errors, so an automatic damage detection technique is needed.

One application of the GLCM and LBP methods is particularly suitable for detecting damage to solar modules, which can aid in solar module maintenance ([Tang et al., 2024](#)). Previous research has applied GLCM to analyze the texture of damage to solar modules caused by several factors. Electrical damage, such as modules burning due to excessive heat, can cause a decrease in energy conversion efficiency. Additionally, physical damage, such as cracks on the surface of solar modules, can also interfere with their performance. Cracks covering only 2% of the panel surface area can cause a decrease in efficiency of around 6%. Furthermore, severe cracks or damage can cause a greater decrease in output, with the potential for up to

20% or more (He et al., 2023). Therefore, a system capable of detecting damage to the surface of solar modules is needed so that appropriate action can be taken. Based on the background described above, this study aims to apply the GLCM and LBP methods to analyze the texture of damage detection on the surface of solar modules. This study is expected to produce an optimal detection model to support solar module maintenance, thereby increasing the efficiency of sustainable solar energy utilization.

Research Method

This study aims to develop a solar module damage detection system based on image texture analysis using the GLCM and LBP methods (Zhang et al., 2025). The research stages consist of data acquisition, data preparation, modeling, evaluation, and deployment.

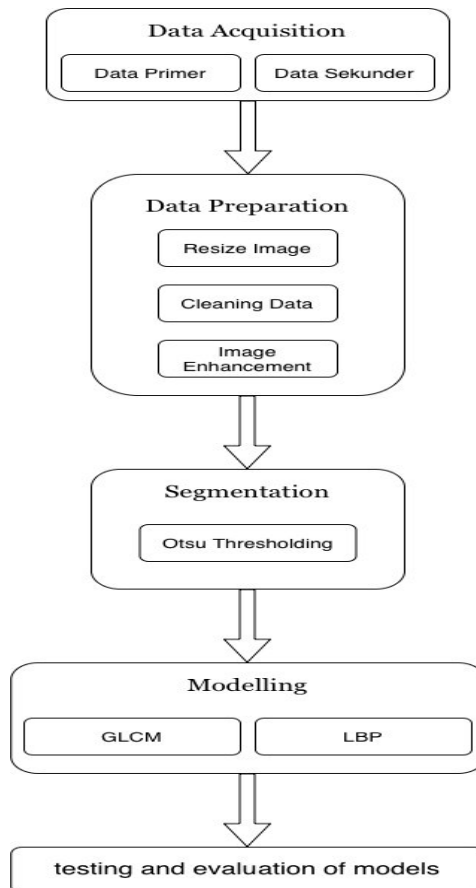


Figure 1 Flowchart of the research method

Data Acquisition

This research incorporates a mix of both primary and secondary data sources to guarantee a wide range and reliability of data. The primary data were sourced directly from a facility at Institut Teknologi PLN, where images of solar panels were taken with a digital camera in a controlled environment. The setup for image capture ensured a consistent distance from the

camera to the module surface (about 30 to 50 centimeters), uniform lighting was utilized to reduce shadows and reflections, and a standard image resolution was maintained to allow for comparisons among different samples. Secondary data were obtained from an openly accessible dataset on Kaggle, chosen for its relevance to the characteristics of solar module damage. The resulting dataset includes 24 images of solar modules with damage. Based on interviews with sources at IT PLN and a literature review ([Barburiceanu et al., 2020](#); [Simon & V., 2020](#)). Various factors can cause damage to solar panel, including extreme weather conditions such as hail, strong winds, or impacts from falling objects. Cracks, breaks, or deformations resulting from physical damage can reduce the performance of solar modules and even cause functional failure. All images are saved in .jpg and .png formats and have been adjusted to a consistent resolution before further processing. The criteria for including images in the dataset are: (1) the solar module surface must be clearly visible, (2) damage characteristics must be recognizable, and (3) the images should have adequate quality regarding contrast and sharpness. The criteria for exclusion are: (1) images that are out of focus, (2) images that contain too much noise or lighting issues, and (3) images that depict incomplete or partially visible solar modules. Ground truth labels were created via a hands-on annotation method that involved visual examination and specific criteria to differentiate between physical and electrical damage traits. The researcher carried out the annotation and confirmed its reliability through multiple rounds of labeling to maintain uniformity. Each image received one class label (either physical or electrical damage) based on its most prominent visual features. Furthermore, an evaluation of image quality was undertaken, which included analyzing resolution, consistency of lighting, and levels of contrast, to verify that the dataset was appropriate for extracting texture features using the GLCM and LBP techniques ([Zhao et al., 2019](#)).

Data Preparation

The data preparation process is carried out so that the image data is ready for use in the analysis and modeling phases. The main objective is to ensure that the data is consistent, neat, and of good visual quality so that it can produce more accurate features. The first step is to resize the images so that they all have the same dimensions, making the subsequent processing more consistent and efficient. Next is data cleaning, which involves reducing visual disturbances or ambiguities that may affect the extraction of information from the image. This stage helps highlight important parts of the image and reduces the influence of external factors such as light differences or unnecessary details ([Lean et al., 2006](#)). After the cleaning process, image enhancement is performed to improve contrast and texture clarity. This is important because it facilitates pattern recognition in images, allowing for more accurate texture feature extraction. By going through these various data preparation stages, the images become more

standardized and ready for further processing in the feature extraction and model analysis phases.

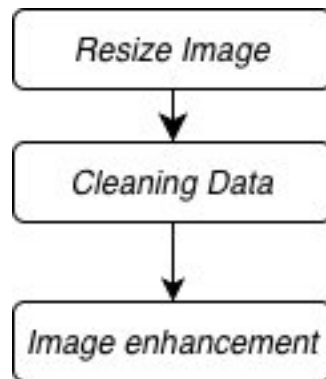


Figure 2 Data Preparation Steps

Resize Image

All images are resized to 100×100 pixels so that they have uniform dimensions and are suitable for GLCM model input requirements. This size was chosen to speed up the training process without losing important texture information. The process begins with selecting the input folder and determining the image size, then the system processes each image file repeatedly, resizing it, and saving the results until all images have been processed.

Cleaning Data

Data cleaning is done by selecting images based on the quality and clarity of the objects. Images with damaged objects that are not clearly visible and duplicate images will be removed to ensure the model remains accurate and to avoid interference during the training process.

Image Enhancement

Image enhancement is a process to improve the visual quality of images, especially in clarifying texture details and pixel intensity differences. Enhancement is performed because some solar module images in the dataset have varying levels of contrast, making damage patterns such as cracks or burnt areas less visible. Through enhancement, the image display becomes sharper and texture variations are more visible, supporting the feature extraction process using the GLCM and LBP methods. During the enhancement stage, image contrast is increased and texture details become clearer. One of the techniques used is Contrast Limited Adaptive Histogram Equalization (CLAHE), which is an adaptive contrast enhancement method that works on small parts of the image so that texture details can be clarified without making the image too bright or too dark. After the enhancement process is complete, the image is saved again and is ready to be used in the texture feature extraction stage.

Segmentation using the Otsu thresholding method

Segmentation is an important part of image analysis where the goal is to clearly separate the area of interest, which is the solar module surface, from the rest of the background. This process removes unnecessary details so that the next step of analyzing texture only looks at important areas. In this study, segmentation is done using the Otsu Thresholding method, which is an automatic global thresholding technique that uses the grayscale intensity histogram. All the images that are used are first made smaller to fit in a 100×100 pixel size. Then, they are cleaned up to remove any unwanted noise, and the contrast is improved using a technique called CLAHE. The images are turned into black and white with 256 different shades of gray to make sure the brightness is shown clearly and evenly.

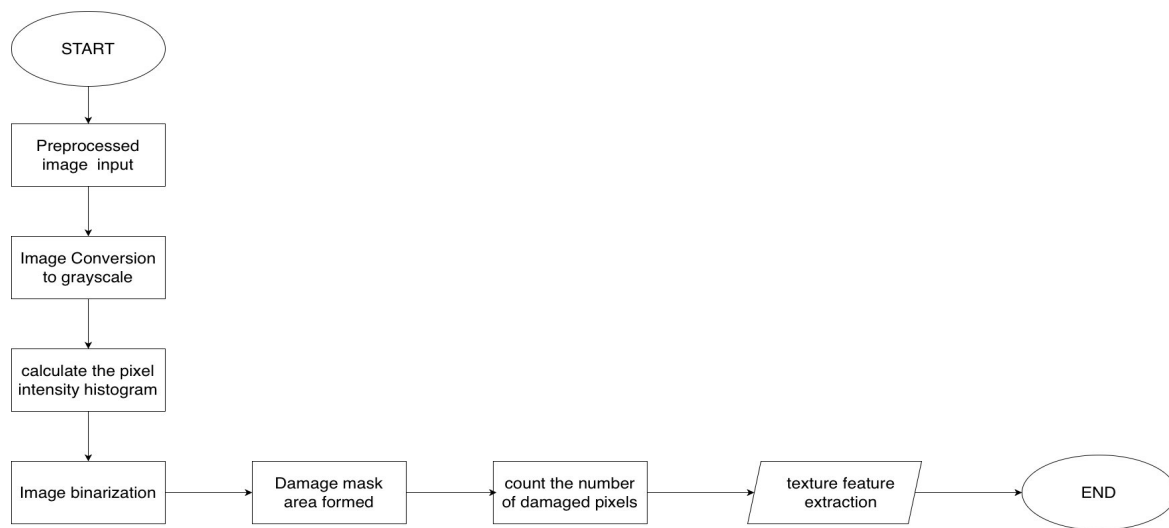


Figure 3 Otsu thresholding segmentation steps

The image analysis process begins with the use of preprocessed images, which have undergone size adjustment, noise cleaning, and image quality enhancement. The images are then converted to grayscale to simplify the visual information so that the analysis focuses on the distribution of pixel intensity. The next step is to calculate the pixel intensity histogram to determine the distribution of gray values. This distribution forms the basis for separating pixels into two classes, namely background and object. The optimal threshold value is determined using the Otsu Thresholding method, which selects the threshold by maximizing the between-class variance:

$$\sigma_b^2(t) = \omega_1(t) \omega_2(t) [\mu_1(t) - \mu_2(t)]^2 \quad (1)$$

where ω_1 and ω_2 are the probabilities of each class, and μ_1 and μ_2 are the average intensities of each class. The t-value that produces the maximum σ_b^2 is selected as the optimal threshold. Once the threshold value is obtained, the image is converted into a binary image using the function:

$$g(x,y) = \begin{cases} 1, & f(x,y) > t \\ 0, & f(x,y) \leq t \end{cases} \quad (2)$$

where $f(x,y)$ is the original pixel intensity and $g(x,y)$ is the segmentation result. Pixels with a value of 1 represent areas that have different texture characteristics and are potentially damaged areas.

Modelling

The modeling stage aims to develop a solar module damage detection system based on texture characteristics by comparing two feature extraction methods, namely GLCM and LBP. Each pre-processed image is converted to grayscale and its contrast is enhanced using the CLAHE method to clarify texture intensity variations. In the LBP method, features are obtained by comparing the intensity of the center pixel to its neighboring pixels to form a local binary pattern. The pattern is represented in the form of a histogram arranged into an $N \times M$ feature matrix, where N is the number of images and M is the number of texture features. All features extracted from GLCM and LBP are used in the clustering process using the K-Means algorithm with the Euclidean distance metric. The value of K is equal to 2 to obtain the best performance. The clustering process is performed separately on GLCM and LBP features so that the two methods can be compared objectively.

Table 1 Hyperparameter Configuration

Distance Metric	Euclidean
K	2
GLCM Parameters	Distance = 1, Angle = 0°-135°
LBP Parameters	Radius (R)=1, Number of Points (P)=8, Histogram Feature

Table 1 shows the hyperparameter configuration used in model training. This evaluation aimed to determine the most optimal texture feature extraction method between GLCM and LBP in detecting damage to solar modules based on digital images. The GLCM algorithm for identifying damage to solar modules.

The GLCM method is used to extract texture characteristics to distinguish between damaged and normal solar module surfaces. The process begins with image acquisition using a digital camera with even lighting, followed by pre-processing in the form of resizing the image to 100×100 pixels and converting RGB to grayscale. Because GLCM is based on gray intensity distribution, contrast enhancement or noise reduction is performed when necessary to clarify texture patterns. The grayscale image is then divided into a 3×4 grid (12 blocks) so that texture analysis can be performed locally, allowing small damage such as cracks or stains to be detected. In each block, a GLCM matrix is formed with a pixel distance of $d=1$, angle

orientations of 0°, 45°, 90°, 135°, and 256 gray levels. The following are the equations used to calculate the contrast, dissimilarity, homogeneity, energy, ASM, X_norm, and damage percentage values used in the study. The following equation represents the frequency of occurrence of pixel pairs with intensities i and j at a certain distance and direction, which is then normalized into the probability of occurrence.

$$P_n(i,j) = \frac{P(i,j)}{\sum_{i,j} P(i,j)} \quad (3)$$

The normalized GLCM matrix calculates statistical texture features. Contrast, which describes local intensity variation, is calculated using the equation,

$$Contrast = \sum_{i,j} (i-j)^2 P_n(i,j) \quad (4)$$

Meanwhile, Dissimilarity, which indicates the degree of pixel dissimilarity, is calculated using the following equation:

$$Dissimilarity = \sum_{i,j} |i-j| P_n(i,j) \quad (5)$$

The homogeneity feature is used to measure texture uniformity, with the equation:

$$Homogeneity = \sum_{i,j} \frac{P_n(i,j)}{1+(i-j)^2} \quad (6)$$

The degree of order in the texture pattern is expressed by the energy and Angular Second Moment (ASM) calculated by,

$$Energy = \sum_{i,j} P_n(i,j)^2 \quad (7)$$

$$ASM = \sum_{i,j} P_n(i,j)^2 \quad (8)$$

The feature values from the four directions are averaged for each block, resulting in a stable texture representation even when faced with changes in orientation. Next, all features are normalized using the Standard Scaler method.

$$X_{norm} = \frac{X-\mu}{\sigma} \quad (9)$$

Before classification using the K-Means Clustering method with k = 2 based on the objective function reduction method. Clusters with the highest contrast levels are considered to be damaged areas. In these areas, segmentation is performed using the Otsu method to find the most appropriate threshold value, thereby increasing the difference between classes.

$$percentage\ of\ damage = \frac{N_{Defect}}{N_{total}} \times 100\% \quad (10)$$

In general, damaged solar module surfaces have a more random texture, resulting in greater contrast and similarity differences, while homogeneity and energy decrease compared to

normal surfaces with a more uniform texture. In this study, the LBP method was used to analyze the texture of solar module surfaces to detect areas of damage. This method was chosen because it effectively represents local texture patterns and is relatively resistant to lighting variations. The process began with image acquisition using a digital camera with uniform lighting, followed by pre-processing in the form of resizing the image to 100×100 pixels and converting it to grayscale so that the analysis only depended on gray intensity. The grayscale image was then divided into a 4×3 grid, resulting in 12 image blocks. This division aims to perform texture analysis locally, so that small damages such as cracks or stains can be detected. In each block, texture features are extracted using the LBP operator. The LBP value of a pixel is calculated by comparing the intensity of the center pixel G_c with the neighboring pixels G_p within a radius of R . The binary value is obtained through a threshold function. Thus, the LBP value is defined as

$$LBP_{P,R} = \sum_{p=0}^{P-1} s(g_p - g_c) \cdot 2^p \quad (11)$$

Where P is the number of neighboring points (in this study, $P = 8$, $R = 1$). The method used is uniform LBP to reduce pattern complexity. From the LBP image in each block, statistical features such as mean, variance, and entropy are calculated. The LBP mean value is calculated as follows.

$$\mu LBP = \frac{1}{N} \sum_{i=1}^N (LBP_i - \mu LBP)^2 \quad (12)$$

And entropy is calculated using

$$Entropy = -\sum_k P_k \log_2 P_k \quad (13)$$

Where P_k is the probability of a particular LBP value appearing. These features are then normalized using Standard Scaler.

$$X_{norm} = \frac{X - \mu}{\sigma} \quad (14)$$

Before classification, features are normalized to standardize the data scale. Next, grouping is performed using the K-Means Clustering algorithm with $k=2$ to separate coarse and normal texture areas. Clusters with higher LBP average values are assumed to be damaged areas. These areas were then segmented using the Otsu method to determine the optimal threshold so that damaged pixels could be separated from normal pixels, and the area of damage could be calculated.

$$Persentase\ kerusakan = \frac{N_{Cacat}}{N_{total}} \times 100\% \quad (15)$$

Evaluation and Testing

This stage aims to assess the extent to which the GLCM method is capable of detecting damage to solar panels based on the results of previous analyses. The assessment is carried out using a Confusion Matrix, which produces several metrics such as Accuracy, Precision, Recall, F1-Score, and Error Rate to measure the accuracy of the system. The results of this evaluation stage are used as a reference to assess the reliability of the model and how consistent and accurate the GLCM method is in providing results.

The final stage is the process of applying the research results in the form of a system or recommendations for using certain methods. At this stage, primary data and assessment results are used to create documents and guidelines for implementing a damage detection system for solar modules using digital image processing techniques. In addition, researchers also provide their analysis results as basic material for further research or the development of automatic monitoring systems that can be applied in the renewable energy industry. With this implementation stage, the research is not only theoretical, but also provides practical benefits in assisting maintenance and improving the efficiency of Solar Power Plants (SPPs).

Result and Discussion

Result

Solar module images used as test data first undergo pre-processing in the form of resizing to 100×100 pixels and contrast enhancement using the CLAHE method. This process aims to clarify texture details before analysis is performed. The image is then divided into a 4×3 grid (12 blocks) so that texture analysis can be performed locally as shown in Figure 4. The block-based approach enables the system to detect minor damage such as cracks, stains, or surface structure disturbances.



Figure 4 Image Resizing and Partitioning Results

Texture features are calculated using the GLCM method with a pixel distance $d = 1$ and angle orientations of 0° , 45° , 90° , and 135° . The extracted parameters include contrast, correlation, energy, and homogeneity. The feature values from each angle are averaged to obtain a texture representation for each block.

Table 2 GLCM feature extraction results with an angle orientation of 0°

experiment	Contrast	Correlation	Energy	Homogeneity
1	3503.077	0.529	0.026	0.033
2	3862.704	0.426	0.027	0.034
3	3842.170	0.378	0.026	0.024
4	2197.969	0.597	0.027	0.034
5	2522.650	0.490	0.027	0.033
6	1754.173	0.766	0.029	0.085

Table 2 shows the results of GLCM feature extraction at an angle orientation of 0° with the highest contrast value in the second experiment at 3862.704, indicating a large variation in intensity due to the rough surface texture. The lowest contrast value was found in the sixth experiment at 1754.173. Meanwhile, for correlation, the highest value was found in the sixth experiment at 0.766, and the lowest value was found in the third experiment at 0.378, indicating low spatial regularity between pixels, which leads to texture disturbance or minor damage. The lowest energy and homogeneity values were found in the third experiment, while the highest values were found in the sixth experiment. The sixth experiment had the lowest contrast value and the highest correlation, energy, and homogeneity values, indicating the smoothest and most horizontally regular texture.

Table 3 GLCM feature extraction results with an angle orientation of 45°

experiment	Contrast	Correlation	Energy	Homogeneity
1	4580.833	0.385	0.027	0.021
2	4474.746	0.322	0.027	0.027
3	4752.086	0.234	0.026	0.020
4	3557.495	0.343	0.027	0.024
5	3211.840	0.351	0.027	0.026
6	7425.679	-0.047	0.027	0.027

Table 3 shows the results of GLCM feature extraction at a 45° angle orientation with the highest contrast value in the sixth experiment at 7425.679, indicating that the diagonal direction is very sensitive in detecting texture changes due to surface damage. The lowest contrast value was found in the fifth experiment at 3211.840. The highest correlation value was found in the first experiment at 0.385, and the lowest correlation value was found in the sixth experiment at -0.047. The negative correlation value in the sixth experiment indicates a highly irregular relationship between pixels, which usually appears in severely damaged areas.

The lowest energy and homogeneity values were found in the third experiment, indicating the most complex and non-homogeneous texture.

Table 4 GLCM feature extraction results with an angle orientation of 90°

experiment	Contrast	Correlation	Energy	Homogeneity
1	3424.410	0.530	0.026	0.033
2	3596.676	0.466	0.027	0.031
3	4056.055	0.348	0.026	0.021
4	2850.091	0.456	0.027	0.032
5	2125.933	0.567	0.027	0.038
6	6042.894	0.128	0.028	0.048

Table 4 shows the results of GLCM feature extraction at a 90° angle orientation with the highest contrast value found in the sixth experiment at 6042.894, indicating strong vertical intensity variation due to cracks or elongated stains, and the lowest value in the fifth experiment at 2125.933. The highest correlation value was found in the fifth experiment at 0.567, indicating that the texture was still relatively regular in the vertical direction. The lowest value was found in the sixth experiment at 0.128. For the energy and homogeneity values, similar to the previous experiment, the lowest value was found in the third experiment, consistent with the previous orientation results, indicating the most random and non-uniform texture.

Table 5 GLCM feature extraction results with an angle orientation of 135°

experiment	Contrast	Correlation	Energy	Homogeneity
1	4579.773	0.384	0.026	0.023
2	4685.720	0.292	0.027	0.025
3	4686.678	0.251	0.026	0.019
4	3317.881	0.387	0.027	0.024
5	3086.942	0.373	0.027	0.028
6	7455.346	-0.049	0.027	0.027

Table 5 shows the results of GLCM feature extraction at an angle of 135°, revealing a pattern similar to that at an angle of 45°, with the highest contrast value again appearing in the sixth experiment with a value of 7455.346. This confirms that the diagonal orientation is very effective in extracting intensity differences in damaged areas. The highest correlation value of 0.387 in the fourth experiment indicates a relatively more regular texture compared to other experiments. In terms of energy and homogeneity values, similar to the previous experiment, the lowest value was found in the third experiment, indicating the dominance of complex textures. The measurement results show a general pattern that:

1. The highest contrast appears at diagonal angles (45° and 135°), indicating large intensity variations in damaged areas.
2. Correlation and homogeneity are higher at 0° and 90° , indicating a more regular normal texture.
3. Relatively low energy, indicating that the surface texture of the module is complex. This pattern is consistent in most experiments (Tables 2–5).

Texture features were normalized using Standard Scaler, then grouped with K-Means Clustering ($k=2$) to separate normal and damaged blocks. Clusters with higher average contrast values were considered damaged areas. The identified damaged blocks were then segmented using the Otsu method to obtain detailed damaged pixels. Texture feature extraction using the Local Binary Pattern (LBP) method with parameters of number of neighbors $P = 8$ and radius $R = 1$ aims to capture local texture patterns on the surface of solar modules in detail. The analysis was performed on four angle orientations (0° , 45° , 90° , and 135°) to accommodate variations in texture direction, so that the information obtained is more robust to changes in image orientation. The extracted statistical parameters include mean, variance, and entropy, which represent the average intensity of local patterns, the level of texture variation, and the complexity of pattern distribution, respectively.

Table 6 LBP feature extraction results with an angle orientation of 0°

Experiment	LBP Mean	LBP Variance	LBP Entropy
1	5.697	9.365	3.063
2	5.651	10.500	3.023
3	5.532	10.819	3.033
4	5.361	9.650	3.164
5	5.332	9.780	3.173
6	5.483	9.603	3.117

Table 6 shows the results of LBP feature extraction with an angle orientation of 0° , where the highest LBP Mean value was found in the first experiment with a value of 5.697 and the lowest value was found in the fifth experiment with a value of 5.332. This shows that the first experiment had more dominant local intensity changes compared to the other experiments. The highest LBP Variance value was found in the third experiment with a value of 10.819, indicating large local texture variations, which are generally associated with surface irregularities. The lowest value was found in the first experiment with a value of 9.361. The highest LBP entropy value was found in the fifth experiment at 3.173, indicating a more complex and random texture pattern distribution, and the lowest LBP entropy value was found in the second experiment at 3.023.

Table 7 LBP feature extraction results with an angle orientation of 45°

experiment	Contrast	Correlation	Energy
1	3503.077	0.529	0.026
2	3862.704	0.426	0.027
3	3842.170	0.378	0.026
4	2197.969	0.597	0.027
5	2522.650	0.490	0.027
6	1754.173	0.766	0.029

Table 7 shows the results of LBP feature extraction with a 45° angle orientation, where the highest LBP Mean value was found in the fifth experiment with a value of 7.351, indicating that this diagonal direction is very sensitive in capturing texture changes due to damage. The lowest value was found in the sixth experiment with a value of 5.748. The highest LBP Variance value was found in the third experiment with a value of 10.301, and the lowest value was found in the fifth experiment with a value of 4.866, indicating the dominance of certain patterns. The highest LBP entropy value was found in the sixth experiment at 3.013, and the lowest LBP entropy value was found in the fifth experiment at 2.300, indicating that even though the texture is rough, the patterns formed tend to be focused and do not spread randomly.

Table 8 LBP feature extraction results with an angle orientation of 90°

Experiment	Contrast	Correlation	Energy
1	3503.077	0.529	0.026
2	3862.704	0.426	0.027
3	3842.170	0.378	0.026
4	2197.969	0.597	0.027
5	2522.650	0.490	0.027
6	1754.173	0.766	0.029

Table 8 shows the results of LBP feature extraction with an angle orientation of 90°. The pattern is similar to the others, where the highest LBP Mean value is found in the fifth experiment with a value of 7.183 and the lowest value is found in the sixth experiment with a value of 5.315. The highest LBP Variance value is found in the sixth experiment with a value of 10.595, and the lowest value is found in the fifth experiment with a value of 5.400. The highest LBP entropy value was found in the sixth experiment at 3.104, and the lowest LBP entropy value was found in the fifth experiment at 2.382, indicating a very uneven and complex texture, which can be associated with damage spreading vertically on the surface of the solar module.

Table 9 LBP feature extraction results with an angle orientation of 135°

experiment	Contrast	Correlation	Energy
1	3503.077	0.529	0.026
2	3862.704	0.426	0.027
3	3842.170	0.378	0.026

4	2197.969	0.597	0.027
5	2522.650	0.490	0.027
6	1754.173	0.766	0.029

Table 9 shows the results of LBP feature extraction with an angle orientation of 135° , where the highest LBP Mean value was again found in the fifth experiment with a value of 7.365 and the lowest value was found in the sixth experiment with a value of 5.706. The highest LBP Variance value is found in the third experiment with a value of 10.370, and the lowest value is found in the fifth experiment with a value of 4.585. The highest LBP entropy value was found in the sixth experiment at 3.027, and the lowest LBP entropy value was found in the fifth experiment at 2.291, indicating a rough texture but with a relatively uniform pattern. This reinforces the finding that diagonal orientation is effective in detecting damage with dominant texture characteristics. The measurement results show a general pattern that:

1. The mean LBP value tends to be higher in damaged areas, indicating sharper local intensity changes due to rough or uneven surface textures.
2. LBP variance shows considerable variation between angles, indicating differences in the distribution of local texture patterns. Normal areas have more balanced pattern variations, while damaged areas show the dominance of certain patterns.
3. LBP entropy is relatively high, indicating that the texture pattern distribution is complex and random. In some damaged areas, entropy decreases slightly because the texture pattern becomes more centered on certain types of patterns due to surface disturbances.

Texture features are calculated using the Local Binary Pattern (LBP) method, then normalized using Standard Scaler so that each feature has a uniform scale. Next, clustering is performed using the K-Means Clustering algorithm with $k=2$ to separate image blocks into two groups, namely blocks with normal texture and blocks containing indications of damage. Clusters with higher average LBP values are interpreted as damaged areas because they show rougher and more uneven local textures. Blocks identified as damaged are then segmented using the Otsu method to obtain more detailed damaged pixels. This segmentation allows the separation of damaged pixels from the background so that the area of damage can be calculated quantitatively.

Discussion

The evaluation was conducted to determine the analysis results based on the texture features obtained using the GLCM and LBP methods. Table 10 shows the results of model testing using GLCM and LBP features. This indicates that texture characteristics measured through the parameters of contrast, correlation, energy, and homogeneity can clearly distinguish between

normal and damaged classes in the feature space. High contrast values in damaged areas and lower homogeneity levels compared to normal areas are the main factors in strengthening the separation between classes.

Table 10 Comparison of GLCM and LBP

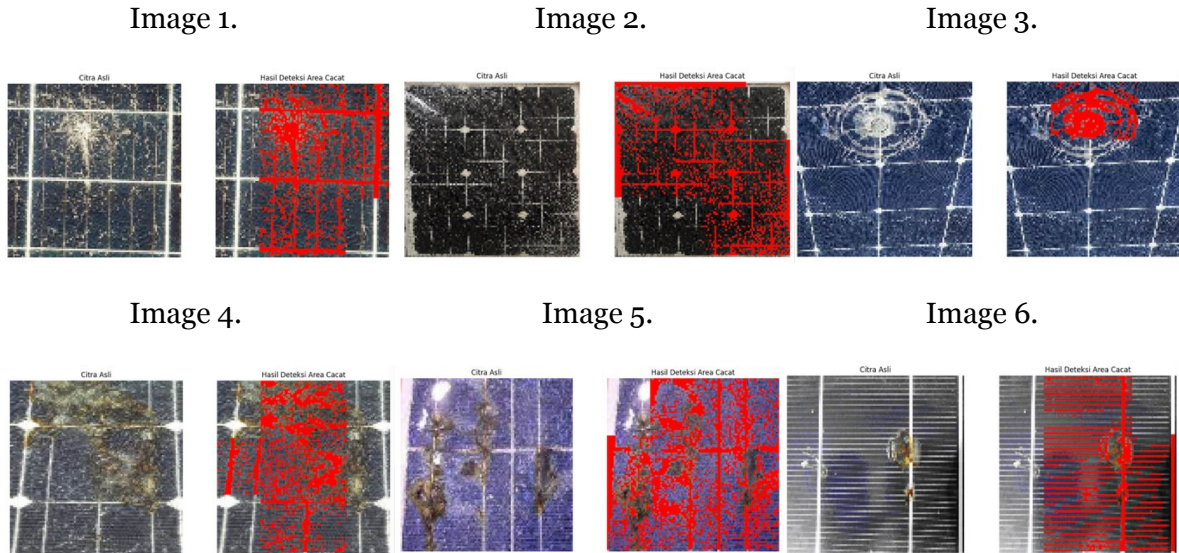
Experiment	Damage GLCM (%)	Damage LBP (%)
1	21.69	23.64
2	22.06	20.65
3	7.93	27.02
4	20.93	15.22
5	19.54	15.80
6	35.78	14.34

Table 10 Shows the segmentation results with varying degrees of damage to the surface of the solar modules in each image. Experiment 6 had the highest percentage of damage (35.78%), indicating widespread and scattered texture disturbances on the surface of the modules. In contrast, image 3 shows the lowest damage percentage (7.93%), indicating that the damage is localized and only occurs in a small area. The other images range from 19 to 22%, indicating moderate damage. These percentages reflect the differences in texture characteristics between images, where areas with high contrast and low homogeneity tend to produce a larger damaged area. This analysis shows that the GLCM-based method is capable of objectively quantifying the level of damage through the calculation of the damaged area.

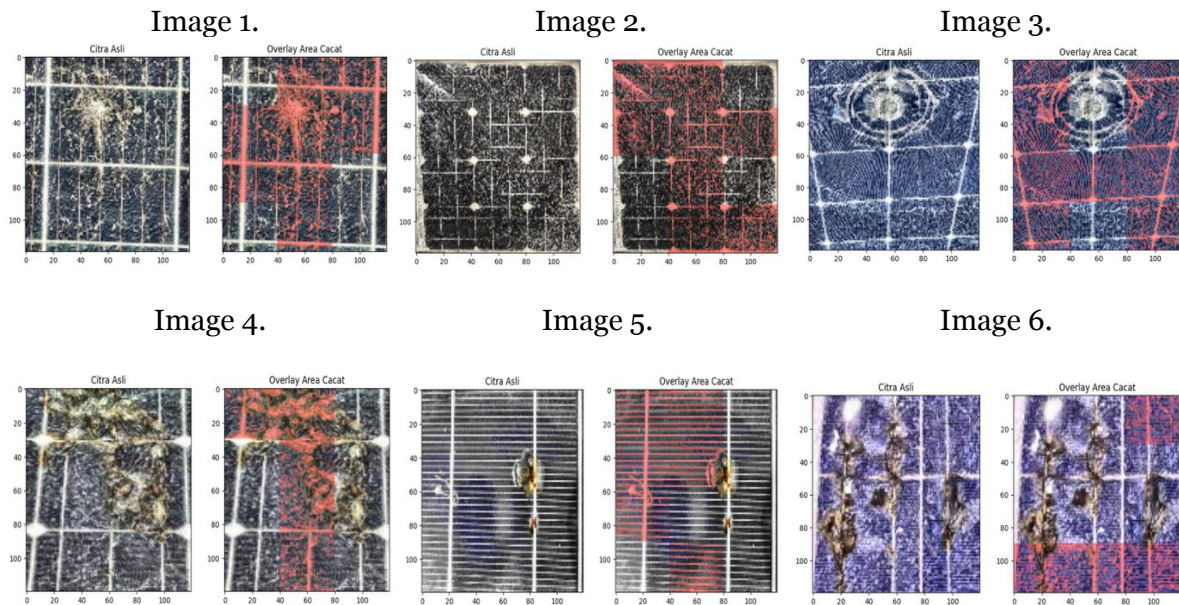
The LBP segmentation results show that the level of damage to the solar module surface varies in each image. Image 3 has the highest percentage of damage (27.02%), indicating that there is widespread and scattered texture disturbance on the module surface. In contrast, image 6 shows the lowest percentage of damage (14.34%), indicating that the damage is more limited and only occurs in some areas. Image 1 (23.64%) and image 2 (20.65%) are classified as moderate to fairly high damage, indicating clear but not comprehensive texture changes. Meanwhile, image 4 (15.22%) and image 5 (15.80%) show a lower level of damage compared to the other images, although they still show local texture disturbance. These percentages reflect the differences in texture characteristics between images, where areas with rougher textures, high pixel intensity variations, and irregular patterns tend to produce larger damaged areas. This analysis shows that texture-based methods are capable of objectively quantifying the level of damage by calculating the area of damage in each image.

The segmentation results show variations in the level of damage between images in both GLCM and LBP. In some images, there are minor errors in grouping, where one piece of data that is actually normal is detected as damaged. However, in general, the accuracy remains stable at 100% damage, which shows that the model is still very reliable. This error occurs

because the texture in normal areas and areas with minor disturbances looks similar, making the feature separation boundaries unclear.



(a) Segmentation in GLCM



(b) Segmentation in LBP

Figure 6 Segmentation Results on (a) GLCM and (b) LBP

Figure 6 Displaying the results of object detection segmentation using the GLCM and LPB methods. Figure 2. (a) shows the ability of GLCM to detect damage more stably in distinguishing the surface condition of solar modules, especially in recognizing texture differences based on the spatial relationship between pixels. Meanwhile, Figure 3. (b) shows the segmentation results of damage detection using LBP. The LBP segmentation results are

better at displaying soft local texture patterns. Combining these two methods provides a complementary approach in the damage detection system for solar modules using digital images. Thus, the evaluation process shows that texture analysis using GLCM and LBP is effective enough to be used as a basis for automatic and objective detection of solar module conditions. Meanwhile, the LBP feature-based model also demonstrates the ability to detect local texture patterns well. The average, variance, and entropy features of LBP can explain changes in texture patterns in areas experiencing damage. Areas with damage usually show higher average LBP values and a more uneven pattern distribution. However, compared to GLCM, LBP features are more sensitive to local pattern changes, resulting in differences in the separation of damaged areas in some situations. Overall, the detection results are still considered good because they are able to consistently distinguish between rough and normal textures.

Conclusions

This study successfully applied texture analysis methods based on the GLCM and LBP to automatically detect surface damage on solar modules using digital images. The test results showed that the GLCM texture feature was able to distinguish between normal and damaged solar modules very well, with the highest damage percentage (35.78%) indicating widespread and scattered texture disturbances on the module surface. Conversely, the lowest damage percentage (7.93%) indicated that the damage was local and only occurred in a small area. The remaining images ranged from 19 to 22%, indicating moderate damage. These percentages reflect differences in texture characteristics between images, where areas with high contrast and low homogeneity tend to produce larger damage areas. This analysis demonstrated that the GLCM-based method was able to objectively measure the extent of damage through the calculation of the damage area, as demonstrated in all experiments. Feature characteristics such as high contrast and homogeneity values and lower energy in the damaged area provided a clear class separation in the feature space. Meanwhile, the LBP method was able to detect local texture patterns quite well, but produced errors due to its sensitivity to slight texture variations in the normal area. The test results obtained the highest percentage of damage (27.02%), indicating the presence of extensive and scattered texture disturbances on the surface of the module. Conversely, the lowest percentage of damage (14.34%), indicating that the damage is more limited and only occurs in several areas, although it still shows local texture disturbances. The next stage is the segmentation process using the Otsu method, successfully separating damaged pixels from normal pixels and objectively measuring the area of damage. Overall, the results of this study indicate that GLCM is superior in terms of stability and accuracy in detecting solar module damage, while LBP serves as a complementary method

in capturing local texture details. This research is expected to be the basis for the development of a reliable solar module condition monitoring system to support maintenance and improve the efficiency of solar energy utilization.

References

- Ali, A., Habib, S., Khan, Z., Thaljaoui, A., Sun, M., & Muhammad, T. (2025). An artificial neural network implementation on novel tetra hybrid nanofluid model: Case study of solar wind turbines. *Engineering Applications of Artificial Intelligence*, *158*, 111459. <https://doi.org/https://doi.org/10.1016/j.engappai.2025.111459>
- Barburiceanu, S., Terebes, R., & Meza, S. (2020, 3-5 Sept. 2020). 3D Texture Feature Extraction and Classification using the BM3DELBP approach. 2020 IEEE 16th International Conference on Intelligent Computer Communication and Processing (ICCP),
- Barburiceanu, S., Terebes, R., & Meza, S. (2021). 3D Texture Feature Extraction and Classification Using GLCM and LBP-Based Descriptors. *Applied Sciences*, *11*(5), 2332.
- Cahyaningtyas, R., Madenda, S., Bertalya, B., & Indarti, D. (2025). Solar module defects classification using deep convolutional neural network [Classification, Deep Convolutional neural network, Solar module, Transfer learning, The failure types]. *2025*, *11*(3), 15. <https://doi.org/10.26555/ijain.v11i3.1818>
- Dhanraj, J. A., Mostafaeipour, A., Velmurugan, K., Techato, K., Chaurasiya, P. K., Solomon, J. M.,...Phoungthong, K. (2021). An Effective Evaluation on Fault Detection in Solar Panels. *Energies*, *14*(22), 7770.
- Dheepak, G., J., A. C., & Vaishali, D. (2024). Brain tumor classification: a novel approach integrating GLCM, LBP and composite features [Methods]. *Frontiers in Oncology*, *Volume 13 - 2023*. <https://doi.org/10.3389/fonc.2023.1248452>
- He, J., Shao, L., Li, Y., Wang, K., & Liu, W. (2023). Pavement damage identification and evaluation in UAV-captured images using gray level co-occurrence matrix and cloud model. *Journal of King Saud University - Computer and Information Sciences*, *35*(9), 101762. <https://doi.org/https://doi.org/10.1016/j.jksuci.2023.101762>
- Kiswanto, K., Hadiyanto, H., & Sedyono, E. (2024). Meat Texture Image Classification Using the Haar Wavelet Approach and a Gray-Level Co-Occurrence Matrix. *Applied System Innovation*, *7*(3), 49.
- Lean, Y., Shouyang, W., & Lai, K. K. (2006). An integrated data preparation scheme for neural network data analysis. *IEEE Transactions on Knowledge and Data Engineering*, *18*(2), 217-230. <https://doi.org/10.1109/TKDE.2006.22>

- Punnappurath, A., Zhao, L., Abdelhamed, A., & Brown, M. S. (2024). Advocating Pixel-Level Authentication of Camera-Captured Images. *IEEE Access*, *12*, 45839-45846. <https://doi.org/10.1109/ACCESS.2024.3381521>
- Rai, R., Lahiri, S., Banerjee, A., Santra, S., Kumar, S., & Mamtani, M. A. (2026). Estimating anisotropy of fracture patterns using gray level Co-occurrence matrix (GLCM) approach: Implication on understanding permeability anisotropy. *Journal of Structural Geology*, *206*, 105661. <https://doi.org/https://doi.org/10.1016/j.jsg.2026.105661>
- Simon, P., & V, U. (2020). Deep Learning based Feature Extraction for Texture Classification. *Procedia Computer Science*, *171*, 1680-1687. <https://doi.org/https://doi.org/10.1016/j.procs.2020.04.180>
- Subeesh, A., & Chauhan, N. (2025). Deep learning based abiotic crop stress assessment for precision agriculture: A comprehensive review. *Journal of Environmental Management*, *381*, 125158. <https://doi.org/https://doi.org/10.1016/j.jenvman.2025.125158>
- Tang, W., Yang, Q., Dai, Z., & Yan, W. (2024). Module defect detection and diagnosis for intelligent maintenance of solar photovoltaic plants: Techniques, systems and perspectives. *Energy*, *297*, 131222. <https://doi.org/https://doi.org/10.1016/j.energy.2024.131222>
- Wan, S., Lee, H. C., Huang, X., Xu, T., Xu, T., Zeng, X.,...Zhou, C. (2017). Integrated local binary pattern texture features for classification of breast tissue imaged by optical coherence microscopy. *Med Image Anal*, *38*, 104-116. <https://doi.org/10.1016/j.media.2017.03.002>
- Wen, H., Li, J., Yu, J., Huang, J., & Liu, B. (2026). Deep learning-based landslides detection improved by the gray level co-occurrence matrix of RGB optical images. *Journal of Rock Mechanics and Geotechnical Engineering*. <https://doi.org/https://doi.org/10.1016/j.jrmge.2025.09.041>
- Zhang, X., Cui, J., Wang, W., & Lin, C. (2017). A Study for Texture Feature Extraction of High-Resolution Satellite Images Based on a Direction Measure and Gray Level Co-Occurrence Matrix Fusion Algorithm. *Sensors*, *17*(7), 1474.
- Zhang, Y., Nie, G., & Wang, D. (2025). Structural health monitoring based on three-dimensional point cloud technology: A systematic review. *Results in Engineering*, *27*, 106552. <https://doi.org/https://doi.org/10.1016/j.rineng.2025.106552>
- Zhao, X., Lin, Y., Liu, L., Heikkilä, J., & Zheng, W. (2019). Dynamic Texture Classification Using Unsupervised 3D Filter Learning and Local Binary Encoding. *IEEE Transactions on Multimedia*, *21*(7), 1694-1708. <https://doi.org/10.1109/TMM.2018.2890362>